ANALYSIS OF COPRIME ARRAYS ON MOVING PLATFORM

Guodong Qin [1], *Moeness G. Amin* [2], *and Yimin D. Zhang* [3]

[1] School of Electronic Engineering, Xidian University, Xian, Shaanxi 710071, China
[2] Center for Advanced Communications, Villanova University, Villanova, PA 19085, USA
[3] Department of Electrical and Computer Engineering, Temple University, Philadelphia, PA 19122, USA
Emails: gdqin@mail.xidian.edu.cn, moeness.amin@villanova.edu, ydzhang@temple.edu

ABSTRACT

Moving platforms enable sparse arrays to assume higher degrees of freedom and lead to increased number of lags. In essence, array motion can fill the holes in the spatial auto-correlation lags associated with a fixed platform and, therefore, increase the number of sources detectable by the same physical array. In this paper, we consider coprime arrays, and assume quasi-stationarity of the environment, where the source locations and waveforms are assumed invariant over array motion of half wavelength. Expressions of the synthetic array comprising the original coprime array and its shifted version are derived. Analysis of the difference co-array corresponding to the combined array positions before and after motion is provided. It is shown that majority, if not all, of the holes in the original array position can be filled by just a small translation shift along the coprime array axis.

Index Terms— Sparse arrays, DOA estimation, difference co-array, coprime array, array motion.

1. INTRODUCTION

Structured sparse arrays are designed independent of the environment and only seek to increase the number of elements in the difference co-arrays. The latter is a representation of the spatial auto-correlation lags that can be estimated from a given array configuration. An increase in the number of lags leads to a corresponding increase of the number of sources that can be estimated. As such, sparse arrays can estimate the direction-of-arrival (DOA) of more sources than the number of physical sensors [1–9]. This property propels a broad use of these arrays in a variety of applications [10–17]. Compared with the minimum redundant array (MRA) [18], the minimum hole array (MHA) [19] and the nested array [2], the coprime array [1] assumes a simple closed-form expression of sensor positions and spacing. It can identify $O(MN)$ uncorrelated sources with $O(M+N)$ sensors using the difference co-array. DOA estimation is implemented by exploiting the unique or consecutive lags [5] in the difference co-array.

Most of the literature on coprime arrays considers a fixed array platform. However, passive and active sensing is typically performed by a sensor array on a moving platform, e.g., air-borne, vehicle mounted, or ship attached. When dealing with an array in motion, one approach is to assume relatively fast changing environment, and carry direction finding at each array position separately. This, however, decomposes the problem into individual DOA estimation problems that are solved independently. On the other hand, in a slowly changing environment, we can assume that source positions, angular directions, and signal temporal structures to be invariant within short time intervals. For a moving platform, coherent measurements can then be collected across each time interval, specifically at the array original and shifted positions. This, in turn, provides an opportunity to collectively produce a difference co-array with a longer span and more contiguous as well as unique lags.

An important work on coprime arrays on moving platforms was considered in [20], where a coprime array with co-prime integers M and N ($N > M$) was used to provide a hole-free co-array over an extended synthetic aperture. It is shown that the coprime array must move as much as $N\lambda/4$ to produce a hole-free co-array, where λ is the signal wavelength. A large value of N requires the signal environment to be stationary over a long time period. This assumption may not be valid in practical situations. In addition, a large array shift results in high data redundancies and increased computational complexity.

In this paper, we exploit array motion to fill the holes in the difference co-arrays which are usually generated with a fixed array position. Unlike previous work [20], we limit the array translation motion to only a half wavelength so that the spatio-temporal characteristics of the environment remain constant over the array translation motion.

The co-array corresponding to the combined positions before and after the half-wavelength array shift is of a longer virtual aperture with a higher number of degrees of freedom compared to those of a single array position. The paper de-

This work was performed while G. Qin was a visiting scholar at the Villanova University. The work of M. G. Amin and Y. D. Zhang was supported in part by the National Science Foundation under Grant No. AST-1547420.

lineates this property and demonstrates through simulation a superior array performance.

We analyze the difference co-array of the synthetic array consisting of the original array and its shifted version for the case where a coprime array merely moves a half wavelength along its axis. It is shown that such motion can fill most, if not all, of the holes, and as such significantly increases both the contiguous and unique lags, enabling estimation of DOA of a large number of sources.

The remainder of the paper is organized as follows. In Section 2, the signal model and synthetic aperture processing are summarized. Section 3 analyzes the difference co-array of the synthetic array. In Section 4, the difference co-arrays and spatial spectra for different values of M and N are presented through simulations. Section 5 concludes the paper.

2. PROBLEM FORMULATION

Consider an L-sensor sparse receive array whose sensor positions are denoted as d_l, $l = 1, 2, \cdots, L$. The first sensor is used as the reference, i.e., $d_1 = 0$. We consider the scenario that the entire array moves along the array direction at a constant velocity v. As illustrated in Fig. 1, the black circle and red rhombus, respectively, represent the sensor positions of the original and the shifted arrays. Denote $s_q(t)$, $q = 1, \cdots, Q$, as the Q uncorrelated far-field sources sampled at $t = T_s,\ 2T_s,\ \cdots,\ L_sT_s$, where T_s is the sampling interval and L_s is the number of snapshots. The arrival angle of the qth source is denoted as θ_q. Because of the assumed small translation motion of the array, the directions of the sources with respect to the sensor array are considered unchanged.

The output of the receive array, at time t, is expressed as

$$\mathbf{x}(t) = \sum_{q=1}^{Q} s_q(t)\exp(-jvt\kappa_q)\mathbf{a}(\theta_q) + \boldsymbol{\varepsilon}(t) = \mathbf{A}\mathbf{s}(t) + \boldsymbol{\varepsilon}(t), \tag{1}$$

where $\mathbf{a}(\theta_q) = [1, \exp(-jd_2\kappa_q),\ \cdots,\ \exp(-jd_L\kappa_q]^T \in \mathbb{C}^{L\times 1}$ is the array steering vector, $\kappa_q = 2\pi\sin(\theta_q)/\lambda$ is defined for notation convenience, and $(\cdot)^T$ denotes transpose. In addition, $\mathbf{s}(t) = [s_1(t)\exp(-jvt\kappa_1), s_2(t)\exp(-jvt\kappa_2), \cdots, s_Q(t)\exp(-jvt\kappa_Q)]^T$ is the signal vector, $\mathbf{A} = [\mathbf{a}(\theta_1), \mathbf{a}(\theta_2), \cdots, \mathbf{a}(\theta_Q)] \in \mathbb{C}^{L\times Q}$ is the array manifold matrix, and $\boldsymbol{\varepsilon}(t) \in \mathbb{C}^{L\times 1}$ is zero-mean complex additive white Gaussian noise vector with covariance matrix $\sigma_\varepsilon^2\mathbf{I}_L$ with $\mathbf{I}_L$ denoting the $L \times L$ identity matrix. At time $t + \tau$, the output of the receive array becomes

$$\begin{aligned}\mathbf{x}(t+\tau) &= \sum_{q=1}^{Q} s_q(t+\tau)\exp(-jvt\kappa_q)\exp(-jv\tau\kappa_q)\mathbf{a}(\theta_q) \\ &\quad +\varepsilon(t+\tau) \\ &= \mathbf{B}\mathbf{s}(t+\tau) + \varepsilon(t+\tau).\end{aligned} \tag{2}$$

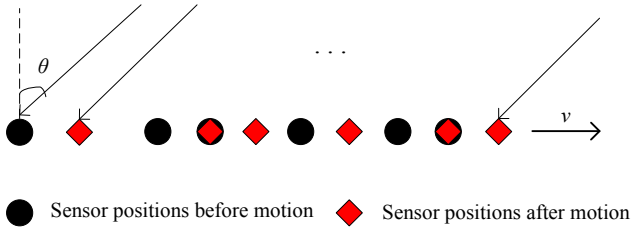

Fig. 1. Array configuration of a moving coprime array.

where

$$\mathbf{B} = [\mathbf{b}(\theta_1), \mathbf{b}(\theta_1), \cdots, \mathbf{b}(\theta_Q)] \in \mathbb{C}^{L\times Q}, \tag{3}$$

with

$$\begin{aligned}\mathbf{b}(\theta_q) &= \exp(-jv\tau\kappa_q)\mathbf{a}(\theta_q) \\ &= [\exp(-jv\tau\kappa_q),\ \exp(-j(v\tau + d_2)\kappa_q), \cdots, \\ &\quad \exp(-j(v\tau + d_L)\kappa_q)]^T,\end{aligned} \tag{4}$$

and

$$\begin{aligned}\mathbf{s}(t+\tau) = [&s_1(t+\tau)\exp(-jvt\kappa_1),\ s_2(t+\tau)\exp(-jvt\kappa_2), \\ &\cdots,\ s_Q(t+\tau)\exp(-jvt\kappa_Q)]^T.\end{aligned} \tag{5}$$

For narrowband signals with carrier frequency f, $s_q(t + \tau) = s_q(t)\exp(j2\pi f\tau)$. Accordingly, (2) can be rewritten as

$$\mathbf{x}(t+\tau) = \exp(j2\pi f\tau)\mathbf{B}\mathbf{s}(t) + \varepsilon(t+\tau). \tag{6}$$

By choosing $v\tau = d = \lambda/2$, the steering vector at time $t + \tau$ becomes

$$\begin{aligned}\mathbf{b}(\theta_q) = [&\exp(-jd\kappa_q),\ \exp(-j(d + d_2)\kappa_q), \cdots, \\ &\exp(-j(d + d_L)\kappa_q)]^T.\end{aligned} \tag{7}$$

By compensating for the phase correction factor $\exp(j2\pi f\tau)$ using the technique described in [21], we obtain a phase synchronized received signal vector as

$$\tilde{\mathbf{x}}(t+\tau) = \mathbf{x}(t+\tau)\exp(-j2\pi f\tau) = \mathbf{B}\mathbf{s}(t) + \tilde{\varepsilon}(t+\tau), \tag{8}$$

where $\tilde{\varepsilon}(t + \tau) = \exp(-j2\pi f\tau)\varepsilon(t + \tau)$.

By combining equations (1) and (8), we obtain the output of the synthetic array. It is expressed as

$$\mathbf{y}(t) = \begin{bmatrix} \mathbf{x}(t) \\ \tilde{\mathbf{x}}(t+\tau) \end{bmatrix} = \mathbf{A}_s\mathbf{s}(t) + \begin{bmatrix} \varepsilon(t) \\ \tilde{\varepsilon}(t+\tau) \end{bmatrix} \in \mathbb{C}^{2L\times 1}, \tag{9}$$

where

$$\mathbf{A}_s = [\mathbf{a}_s(\theta_1), \mathbf{a}_s(\theta_2), \cdots, \mathbf{a}_s(\theta_Q)] \in \mathbb{C}^{2L\times Q}, \tag{10}$$

$$\mathbf{a}_s(\theta_q) = [\mathbf{a}^T(\theta_q), \mathbf{b}^T(\theta_q)]^T. \tag{11}$$

3. DIFFERENCE CO-ARRAY

In this section, we analyze the difference co-array of the synthetic array. We refer to the arrays at its original and shifted positions as the original and shifted arrays, respectively. For a coprime array with coprime integers M and N ($M < N$), the sensor positions are expressed as [5]

$$\mathbb{P}_{co} = \{Mnd, n \in [0, N-1]\} \cup \{Nmd, m \in [0, M-1]\}, \tag{12}$$

whereas the sensor positions of the shifted array are expressed as

$$\mathbb{P}_{cs} = \{(Mn+1)d\} \cup \{(Nm+1)d\}. \tag{13}$$

Combining the sensor positions of the original and the shifted arrays, we obtain the sensor positions of the synthetic array,

$$\mathbb{P}_{c} = \mathbb{P}_{co} \cup \mathbb{P}_{cs}. \tag{14}$$

The synthetic array is illustrated in Fig. 2, where black circles and red rhombuses represent the original and the shifted coprime arrays, respectively. The set formed from the difference co-array corresponding to the synthetic array is given as

$$\mathbb{S}_{\rm c} = \mathbb{S}_{12} \cup \mathbb{S}_{34} \cup \mathbb{S}_{13} \cup \mathbb{S}_{24} \cup \mathbb{S}_{14} \cup \mathbb{S}_{23}. \tag{15}$$

In the above expression, subscripts 1 and 2 refer to the two subarrays in their original positions, whereas 3 and 4 refer to these subarrays in the shifted positions. It is noted that only the cross-lags in the difference co-array are considered here since the self-lag positions form a subset of the cross-lag positions [5].

$\mathbb{S}_{12}$ is defined as the set of cross-lags between original subarray 1 and original subarray 2 which is given [5] as,

$$\mathbb{S}_{12} = \{Mk_1 - Nk_2\} \cup \{Nk_2 - Mk_1\}, \tag{16}$$

where $k_1 \in [0, N-1], k_2 \in [0, M-1]$. Similarly,

$$\mathbb{S}_{34} = \{Mk_3 - Nk_4\} \cup \{Nk_4 - Mk_3\}, \tag{17}$$

where $k_3 \in [0, N-1], k_4 \in [0, M-1]$. From (16) and (17), it is clear that $\mathbb{S}_{12} \cup \mathbb{S}_{34} = \mathbb{S}_{12}$ since $\mathbb{S}_{12}$ and $\mathbb{S}_{34}$ have the same elements. On the other hand, $\mathbb{S}_{13}$ is defined as the set of cross-lags between subarray 1 and subarray 3, whereas $\mathbb{S}_{24}$ is defined as that between subarray 2 and subarray 4. They are, respectively, given as,

$$\mathbb{S}_{13} = \{Mk_1 - Mk_3 - 1\} \cup \{Mk_3 - Mk_1 + 1\}, \tag{18}$$
$$\mathbb{S}_{24} = \{Nk_2 - Nk_4 - 1\} \cup \{Nk_4 - Nk_2 + 1\}. \tag{19}$$

Similarly,

$$\mathbb{S}_{14} = \{Mk_1 - Nk_4 - 1\} \cup \{Nk_4 - Mk_1 + 1\}, \tag{20}$$
$$\mathbb{S}_{23} = \{Nk_2 - Mk_3 - 1\} \cup \{Mk_3 - Nk_2 + 1\}. \tag{21}$$

Lemma 1: For sets $\mathbb{S}_{13}$, $\mathbb{S}_{24}$, $\mathbb{S}_{14}$ and $\mathbb{S}_{23}$ defined above, $\mathbb{S}_{13} \cup \mathbb{S}_{24} \cup \mathbb{S}_{14} \cup {}_{23} = \mathbb{S}_{14} \cup \mathbb{S}_{23}$.

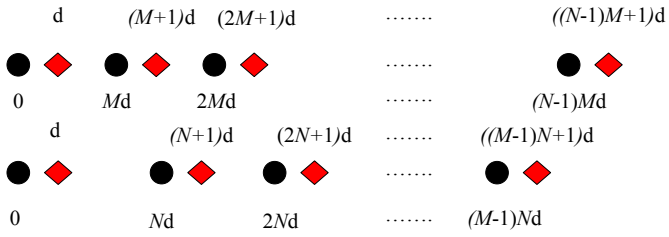

Fig. 2. The two subarrays of the synthetic coprime array.

Proof. See Reference [22]. □

Utilizing Lemma 1 and using the fact that $\mathbb{S}_{12} \cup \mathbb{S}_{34} = \mathbb{S}_{12}$, the cross-lag set of the synthetic array is simplified as

$$\mathbb{S}_{\rm c} = \mathbb{S}_{12} \cup \mathbb{S}_{14} \cup \mathbb{S}_{23}. \tag{22}$$

With different combinations of the subsets, it is easy to show

$$\mathbb{S}_{14} \cup \mathbb{S}_{23} = \tilde{\mathbb{S}}_{14} \cup \tilde{\mathbb{S}}_{23}, \tag{23}$$

where

$$\tilde{\mathbb{S}}_{14} = \{Mk_1 - Nk_4 - 1\} \cup \{Nk_2 - Mk_3 - 1\}, \tag{24}$$
$$\tilde{\mathbb{S}}_{23} = \{Nk_4 - Mk_1 + 1\} \cup \{Mk_3 - Nk_2 + 1\}. \tag{25}$$

Because $k_1, k_3 \in [0, N-1]$, $k_2, k_4 \in [0, M-1]$, (24) and (25) are equivalent to the following equations.

$$\mathbb{S}^{\rm L}_{12} = \{Mk_1 - Nk_2 - 1\} \cup \{Nk_2 - Mk_1 - 1\}, \tag{26}$$
$$\mathbb{S}^{\rm R}_{12} = \{Nk_2 - Mk_1 + 1\} \cup \{Mk_1 - Nk_2 + 1\}. \tag{27}$$

Then,

$$\mathbb{S}_{\rm c} = \mathbb{S}_{12} \cup \mathbb{S}^{\rm L}_{12} \cup \mathbb{S}^{\rm R}_{12}. \tag{28}$$

We remark that the new subsets $\mathbb{S}^{\rm L}_{12}$ and $\mathbb{S}^{\rm R}_{12}$ can be interpreted as the difference co-array of the original coprime array shifted by one unit step (lag) to the left and one unit step to the right. Accordingly, the close neighbouring holes of each lag in the difference co-array of the original coprime array become filled, which makes the number of unique lags increase.

Example 1. Assume $M = 4$, $N = 5$, then $\mathbb{S}_{12} = \{0, \pm1, \cdots, \pm8, \pm10, \pm11, \pm12, \pm15, \pm16\}$. There are 27 unique lags and 6 holes locating at $\{\pm9, \pm13, \pm14\}$. After array motion, there are new subsets $\mathbb{S}^{\rm L}_{12} = \{0, \pm1, \cdots, \pm7, -8, \pm9, 10, \pm11, -12, -13, 14, 15, -16, -17\}$ and $\mathbb{S}^{\rm R}_{12} = \{0, \pm1, \cdots, \pm7, 8, \pm9, -10, \pm11, 12, 13, -14, -15, 16, 17\}$. Therefore, $\mathbb{S}_{\rm c} = \{0, \pm1, \cdots, \pm17\}$. The difference co-array becomes a hole-free array, and the number of unique lags is increased to 35 from 27.

This example shows that the new subsets $\mathbb{S}^{\rm L}_{12}$ and $\mathbb{S}^{\rm R}_{12}$ fill 6 holes in $\mathbb{S}_{12}$ by shifting a coprime array with $M = 4$, $N = 5$ by a half wavelength. Meanwhile, additional 2 lags (±17) are obtained. It is noted that the difference co-array in this case is a hole-free array with motion owing to the fact that all the holes are located at the neighbouring positions of the filled lags.

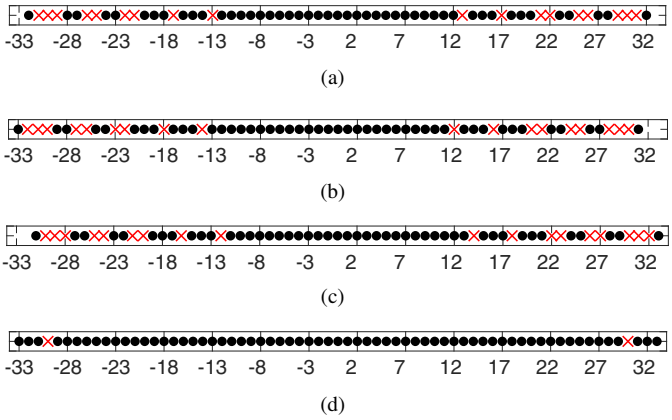

Fig. 3. Difference co-array for M=4, N=9. (a) $\mathbb{S}_{12}$; (b) $\mathbb{S}_{12}^{\mathrm{L}}$; (c) $\mathbb{S}_{12}^{\mathrm{R}}$; (d) $\mathbb{S}_{\mathrm{c}}$.(•: lags; ×: holes)

4. SIMULATION RESULTS

In this section, we analyze the difference co-arrays and spatial spectra estimation performance for the original and synthetic coprime array through numerical simulations.

In the first simulation, the difference co-arrays of the original and synthetic coprime array for M=4, N=9 are analyzed in Fig. 3. The difference co-array $\mathbb{S}_{12}$ corresponding to the original coprime array is shown in Fig. 3 (a). There are 18 holes in the co-array before motion. After motion, the neighbouring holes of each lag are filled by subsets $\mathbb{S}_{12}^{\mathrm{L}}$ and $\mathbb{S}_{12}^{\mathrm{R}}$ (see Fig. 3 (b) and Fig. 3 (c)). Fig.3 (d) depicts the difference co-array of the synthetic array. The reason it is not filled is that there are 3 consecutive holes in the difference co-array of the original array out of which two holes are filled by motion. After motion, the middle one locating at position ± 30 in the 3 consecutive holes is left. Even so, the number of unique lags increases significantly with array shift.

In the second simulation, the spatial spectra estimation results using LASSO [23, 24] for different values of M and N are shown in Fig. 4. $L = 12$ sensors are used for the three arrays with M=4, N=9 and M=6, N=7 as well as M=5, N=8. The numbers of unique lags increase to 65, 69 and 73 after motion from their respective original values 47, 53 and 51, respectively. The input signal-to-noise ratio (SNR) is 10 dB and 2,000 snapshots are used. Q sources are uniformly distributed between -50° and 50°. Different values of Q are considered for each array. Figs. 4(a), 4(c) and 4(e) are for the original array, whereas Figs. 4(b), 4(d), and 4(f) represent the synthetic array. It is evident from Fig. 4 that the original coprime array cannot identify the DOAs of all Q sources, whereas the synthetic coprime array can resolve all sources.

5. CONCLUSIONS

In a relatively slowly changing environment, the number and locations of sources in the field of view of a multi-antenna receiver can be assumed constant over a short period of time. If the receiver implements a sparse array, then by virtue of motion, the original and new positions of the array will together mass a higher number of degrees of freedom than those corresponding to one array position. In this paper, we considered coprime array, and analyzed the co-array of the combined array positions. It was shown that an array motion, through a half wavelength shift, fills most of the holes associated with the coprime array at a fixed position. Specifically, we demonstrated that, by shifting the physical sparse array by half wavelength along its axis, the difference co-array of the combined two array positions would consist of the difference co-array of the original array and its unit-lag shifted versions in the direction and opposite to direction of motion. These additional lags were used to improve the DOA estimation of a large number of sources. The increased number of lags due to array motion is not confined to coprime arrays, and other sparse array structures can similarly benefit from shifting the array by a small displacement.

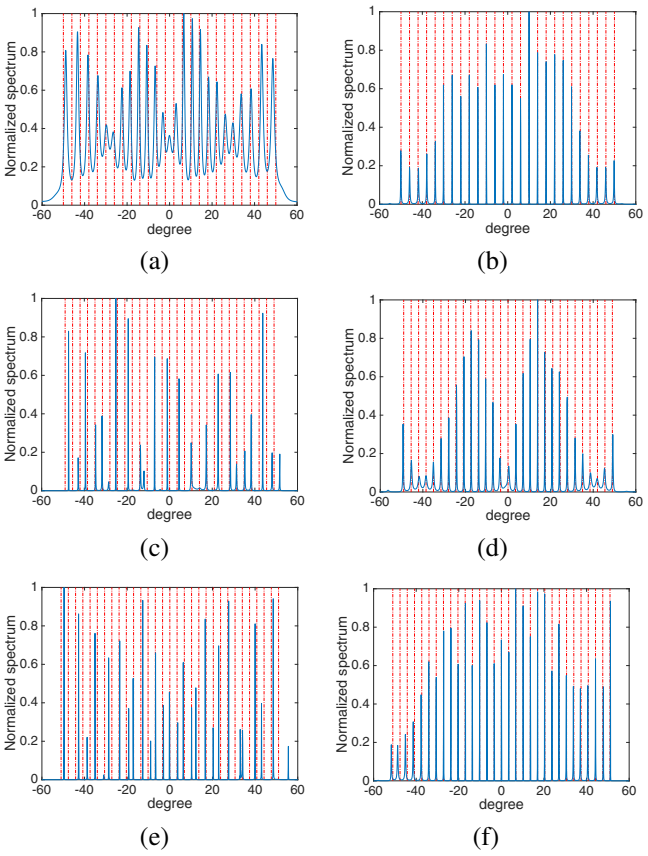

Fig. 4. Spatial spectra estimation using the LASSO. (a) M=4, N=9, Q=26 for the original array; (b) M=4, N=9, Q=26 for the synthetic array; (c) M=6, N=7, Q=29 for the original array; (d) M=6, N=7, Q=29 for the synthetic array; (e) M=5, N=8, Q=31 for the original array; (f) M=5, N=8, Q=31 for the synthetic array.

6. REFERENCES

[1] P. P. Vaidyanathan and P. Pal, "Sparse sensing with co-prime samplers and arrays," *IEEE Trans. Signal Process.*, vol. 59, no. 2, pp. 573–586, February 2011.

[2] P. Pal and P. P. Vaidyanathan, "Nested arrays: A novel approach to array processing with enhanced degrees of freedom," *IEEE Trans. Signal Process.*, vol. 58, no. 8, pp. 4167–4181, August 2010.

[3] C. Liu and P. P. Vaidyanathan, "Remarks on the spatial smoothing step in coarray music," *IEEE Signal Process. Lett.*, vol. 22, no. 9, pp. 1438–1442, September 2015.

[4] Y. D. Zhang, M. G. Amin, and B. Himed, "Sparsity-based DOA estimation using co-prime arrays," in *Proc. IEEE Int. Conf. Acoustics, Speech and Signal Process. (ICASSP)*, May 2013, pp. 3967–3971.

[5] S. Qin, Y. D. Zhang, and M. G. Amin, "Generalized coprime array configurations for direction-of-arrival estimation," *IEEE Trans. Signal Process.*, vol. 63, no. 6, pp. 1377–1390, March 2015.

[6] Z. Tan and A. Nehorai, "Sparse direction of arrival estimation using co-prime arrays with off-grid targets," *IEEE Signal Process. Lett.*, vol. 21, no. 1, pp. 26–29, January 2014.

[7] W. Wang, S. Ren, and Z. Chen, "Unified coprime array with multi-period subarrays for direction-of-arrival estimation," *Digital Signal Process.*, vol. 74, pp. 30–42, 2018.

[8] H. Huang, B. Liao, C. Guo, and J. Huang, "Sparse representation based DOA estimation using a modified nested linear array," in *2018 IEEE Radar Conf.*, April 2018, pp. 919–922.

[9] C. Liu and P.P. Vaidyanathan, "Cramrrao bounds for co-prime and other sparse arrays, which find more sources than sensors," *Digital Signal Process.*, vol. 61, pp. 43–61, 2017.

[10] M. Yang, L. Sun, X. Yuan, and B. Chen, "A new nested MIMO array with increased degrees of freedom and hole-free difference coarray," *IEEE Signal Process. Lett.*, vol. 25, no. 1, pp. 40–44, January 2018.

[11] Y. Gu, C. Zhou, N. A. Goodman, W. Z. Song, and Z. Shi, "Coprime array adaptive beamforming based on compressive sensing virtual array signal," in *Proc. IEEE Int. Conf. Acoustics, Speech and Signal Process. (ICASSP)*, March 2016, pp. 2981–2985.

[12] K Adhikari, J.R. Buck, and K.E Wage, "Beamforming with extended coprime sensor arrays," in *Proc. IEEE Int. Conf. Acoustics, Speech and Signal Process.(ICASSP)*, 2013, pp. 4183–4186.

[13] K. Sun, Y. Liu, H. Meng, and X. Wang, "Adaptive sparse representation for source localization with gain/phase errors," *Sensors*, vol. 11, no. 5, pp. 4780–4793, May 2011.

[14] Y. Gu, Y. D. Zhang, and N. A. Goodman, "Optimized compressive sensing-based direction-of-arrival estimation in massive MIMO," in *Proc. IEEE Int. Conf. Acoustics, Speech and Signal Process. (ICASSP)*, March 2017, pp. 3181–3185.

[15] X. Wang, M. Amin, and X. Cao, "Analysis and design of optimum sparse array configurations for adaptive beamforming," *IEEE Trans. Signal Process.*, vol. 66, no. 2, pp. 340–351, January 2018.

[16] A. Hassanien, M. W. Morency, A. Khabbazibasmenj, S. A. Vorobyov, J. Park, and S. Kim, "Two-dimensional transmit beamforming for mimo radar with sparse symmetric arrays," in *Proc. IEEE Radar Conf.*, April 2013, pp. 1–6.

[17] M. G. Amin, P.P. Vaidyanathan, Y. D. Zhang, and P. Pal, "Editorial for coprime special issue," *Digital Signal Process.*, vol. 61, pp. 1–2, February 2017.

[18] A. Moffet, "Minimum-redundancy linear arrays," *IEEE Trans. Antennas Propagat.*, vol. 16, no. 2, pp. 172–175, March 1968.

[19] D. A. Linebarger, I. H. Sudborough, and I. G. Tollis, "Difference bases and sparse sensor arrays," *IEEE Trans. Inform. Theory*, vol. 39, no. 2, pp. 716–721, March 1993.

[20] J. Ramirez and J. L. Krolik, "Synthetic aperture processing for passive co-prime linear sensor arrays," *Digital Signal Process.*, vol. 61, pp. 62–75, 2017.

[21] S. Stergios and E. J. Sullivan, "Extended towed array processing by an overlap correlator," *J. Acoust. Soc. America*, vol. 86, no. 1, pp. 158–171, 1989.

[22] G. Qin, M. G. Amin, and Y. D. Zhang, "DOA estimation exploiting sparse array motions," under review.

[23] R. Tibshirani, "Regression shrinkage and selection via the lasso," *J. Royal Stat. Soc. Series B*, vol. 58, no. 1, pp. 267–288, 1996.

[24] P. Pal and P. P. Vaidyanathan, "On application of LASSO for sparse support recovery with imperfect correlation awareness," in *Conf. Record of Asilomar Conf. Signals, Systems and Computers*, November 2012, pp. 958–962.